Edinburgh Research Explorer

Reactions of a P–N stabilised aluminium dihydride with ruthenium hydride complexes

OPEN ACCESS
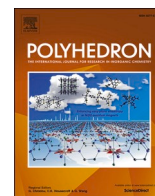
Reactions of a P—N stabilised aluminium dihydride with ruthenium hydride complexes

Anne-Frédérique M. Pécharman [a], Rosalyn L. Falconer [b,c], Esme Owen [a], Michael J. Cowley [b,*], John P. Lowe [a], Claire L. McMullin [a,*], Mary F. Mahon [a], Michael K. Whittlesey [a,*]

[a] Department of Chemistry, University of Bath, Bath BA2 3QD, UK
[b] School of Chemistry, University of Edinburgh, Joseph Black Building, David Brewster Road, Edinburgh EH9 3FJ, UK
[c] Present Address: Department of Chemistry, University of British Columbia, Vancouver, British Columbia V6T 1Z1, Canada

ARTICLE INFO

ABSTRACT

Treatment of $[Ru(L)(PPh_3)_2(CO)H_2]$ (L = PPh_3, IMes; IMes = 1,3-bis(2,4,6-trimethylphenyl)imidazol-2-ylidene) with an *N*-mesityl amidophosphine aluminium dihydride complex (Al(P—N)H$_2$) gives $[Ru(PPh_3)_2(CO)H_3\{Al(P—N)H\}]$ (**2**) and $[Ru(IMes)(PPh_3)(CO)H_3\{Al(P—N)H\}]$ (**4**), which are present in solution as mixtures of diastereomers. Crystal structure determinations and density functional theory (DFT) calculations suggest both **2** and **4** can be formulated as $[Ru(L)(PPh_3)(CO)H_3][Al(P—N)H]$ complexes with bridging hydride ligands.

1. Introduction

Addition of a main group metal alkyl reagent to a transition metal-hydride complex, with subsequent elimination of an alkane, provides a well-established route to transition metal-main group metal (TM-MGM) heterobimetallic complexes [1–5]. Such compounds are potentially also accessible upon loss of H_2 from the combination of a transition metal-hydride precursor and a molecular MGM-hydride although, to date, relatively few studies of this reaction have been undertaken, most likely because of the perceived 'frailty' of MGM-hydrides [6], which has limited their accessibility in comparison to their commercially available alkyl counterparts. However, with the emergence of new molecular MGM-hydrides [7] stabilised by bulky, often chelating ligands, reaction studies with TM-H precursors have begun to appear. Scheme 1 shows some recent results from the Crimmin group on the reactivity of β-diketiminate stabilised Mg, Zn and Al hydrides with Zr, Ru and Rh hydrides [8–11]. In all cases, H_2 elimination does not take place, but instead, there is incorporation of the MGM-H into the coordination sphere of the TM, possibly due to use of an unsaturated TM-H precursor (in the formation of **I**) or the presence of labile leaving groups on the TM (N_2 in **II**, Et_3SiH in **III**) [12–16].

In an attempt to add further to this area, we turned to the ruthenium precursors $[Ru(L)(PPh_3)_2(CO)H_2]$ (L = PPh_3, IMes; Schemes 2 and 3), which are similar to $[Ru(PCy_3)_2(N_2)_2H_2]$ used in the formation of **II** in

Scheme 1 [11], but which feature less labile ligands. For the main group metal hydride, we have employed the recently reported aluminium dihydride compound **1** [17], which features an unusual P—N chelate, rather than the more common N—N based stabilising ligands shown in Scheme 1. Moreover, to date, **1** has not been utilised in any reactions with transition metal complexes.

2. Material and methods

2.1. General comments

All manipulations were carried out under argon using standard Schlenk, high vacuum and glovebox techniques using dry and degassed solvents. C_6D_6 and $C_6D_5CD_3$ were vacuum transferred from potassium. NMR spectra were recorded on Bruker Avance 400 and 500 MHz NMR spectrometers and referenced as follows: C_6D_6 (^{1}H, δ 7.16 ppm; ^{13}C, δ 128.0 ppm) and $C_6D_5CD_3$ (^{1}H, δ 2.09 ppm). ^{31}P{^{1}H} spectra were referenced externally to 85% H_3PO_4 (δ 0.0 ppm). IR spectra of solid samples were recorded on a Bruker ALPHA ATR-IR spectrometer. Elemental analyses were performed by Elemental Microanalysis Ltd, Okehampton, Devon, U.K. Literature methods were employed for the preparation of **1** [17], $[Ru(PPh_3)_3(CO)H_2]$ [18], $[Ru(IMes)(PPh_3)_2(CO)H_2]$ [19], $[Ru(PPh_3)(dppp)(CO)H_2]$ [20], $[Ru(PPh_3)_3(CO)HCl]$ [21] and $[Ru(PPh_3)_3HCl]$ [22].

* Corresponding authors.
E-mail addresses: m.k.whittlesey@bath.ac.uk, deposit@ccdc.cam.ac.uk (M.K. Whittlesey).

2.2. Synthesis of [Ru(PPh₃)₂(CO)H₃{Al(P—N)H}] (2)

A toluene (3 mL) solution of [Ru(PPh₃)₃(CO)H₂] (60 mg, 0.065 mmol) and **1** (26 mg, 0.065 mmol) was heated for 18 h at 60 °C in a J. Young's resealable ampoule. Upon cooling to room temperature, the solution was concentrated by ca. 50% and layered with hexane to give colourless crystals of **2** (36 mg, 52% yield). Redissolution in C₆D₆ for NMR analysis showed the presence of a major and minor diastereomer (designated as 'maj' and 'min' below) in a ratio of ca. 1.7:1. Resonances for the two species overlapped in some cases, leading to non-integer values for integrals. ¹H NMR (500 MHz, C₆D₆, 298 K): δ 7.43–7.33 (m, 22H, Ar$_{maj+min}$), 7.32–7.24 (m, 9H, Ar$_{maj+min}$), 7.00–6.87 (m, 54H, Ar$_{maj+min}$), 6.81 (br s, 1H, Ar$_{min}$), 6.59 (br s, 1.7H, Ar$_{maj}$), 5.37 (br s, 2.7H, AlH$_{maj+min}$), 3.08 (s, 1.7H, CN$_{bridge}$H$_{maj}$), 2.97 (s, 1H, CN$_{bridge}$H$_{min}$), 2.50 (s, 5.1H, C₆H₂$Me_3$$_{maj}$), 2.48 (s, 1H, CP$_{bridge}H_{min}$), 2.45 (s, 1.7H, CP$_{bridge}H_{maj}$), 2.44 (s, 3H, C₆H₂$Me_3$$_{maj}$), 2.27 (s, 3H, C₆H₂$Me_3$$_{maj}$), 2.22 (s, 8.1H, C₆H₂$Me_3$$_{maj+min}$), 1.85 (s, 5.3H, C₆H₂$Me_3$$_{maj}$), 1.74–1.64 (m, 8.3H, C$H_2$$_{maj+min}$), 1.42–1.37 (app. t, ³$J_{HP}$ = 13.6 Hz + d, ³J_{HP} = 13.0 Hz, 44.2H, C$Me_3$$_{maj}$ + C$Me_3$$_{min}$ + CH), 1.23 (d, ³J_{HP} = 13.4 Hz, 9H, C$Me_3$$_{min}$), 1.15 (d, J = 7.5 Hz, 1H, C$H_2$$_{min}$), 1.14 (d, J = 7.7 Hz, 1.7H, C$H_2$$_{maj}$), −8.02 (br s, 2.7H, RuH$Al$$_{maj+min}$), −9.63 (br m, 5.7H, RuH$Al$$_{maj+min}$) ppm. ³¹P{¹H} NMR (202 MHz, C₆D₆, 298 K): δ 49.6–47.2 (m, Ru-$P$$_{maj+min}$), 0.3 (br s, Al-$P$$_{min}$), −0.9 (br s, Ap-$P$$_{maj}$) ppm. ¹³C{¹H} DEPTQ NMR (126 MHz, C₆D₆, 298 K): δ 206.2 (t, ²J_{CP} = 10 Hz, Ru-CO$_{maj}$), 205.7 (t, ²J_{CP} = 9 Hz, Ru-CO$_{min}$), 181.7 (d, J_{CP} = 21 Hz, NCCH$_{maj}$), 181.5 (d, J_{CP} = 20 Hz, NCCH$_{min}$), 144.7 (d, J_{CP} = 3 Hz, NC_{ipso}Mes$_{maj}$), 144.2 (d, J_{CP} = 3 Hz, NC_{ipso}Mes$_{min}$), 139.1 (d, ¹J_{CP} = 35 Hz, P$C_{ipsomin}$), 139.0 (d, ¹J_{CP} = 35 Hz, P$C_{ipsomaj}$), 138.8 (d, ¹J_{CP} = 36 Hz, P$C_{ipsomaj}$), 138.5 (d, ¹J_{CP} = 38 Hz, P$C_{ipsomin}$), 137.6 (s, C_{quat}Mes$_{min}$), 137.0 (s, C_{quat}Mes$_{maj}$), 136.7 (s, C_{quat}Mes$_{min}$) 136.4 (s, C_{quat}Mes$_{maj}$), 134.4 (d, J_{CP} = 13 Hz, CH$_{min}$), 134.3 (d, J_{CP} = 13 Hz, CH$_{maj}$), 134.1 (d, J_{CP} = 11 Hz, CH$_{min}$), 134.0 (d, J_{CP} = 13 Hz, CH$_{maj}$), 133.0 (s, C_{quat}Mes$_{min}$), 132.6 (s, C_{quat}Mes$_{maj}$), 130.0 (s, CH), 129.1 (d, J_{CP} = 6 Hz, CH), 129.0 (s, CH), 128.9 (s, CH), 128.7 (s, CH), 82.1 (d, ¹J_{CP} = 38 Hz, PCCH$_{maj}$), 81.7 (d, ¹J_{CP} = 40 Hz, PCCH$_{min}$), 49.1 (d, ³J_{CP} = 4 Hz, CHCH₂CH$_{min}$), 48.2 (s, CHCH₂CH$_{maj}$), 44.8 (d, ³J_{CP} = 3 Hz, NCCH$_{maj}$), 44.6 (d, ³J_{CP} = 3 Hz, NCCH$_{min}$), 44.5 (d, ²J_{CP} = 8 Hz, PCCH$_{maj}$), 44.3 (d, ²J_{CP} = 8 Hz, PCCH$_{min}$), 36.1 (d, ¹J_{CP} = 15 Hz, PCMe$_{maj}$), 34.7 (d, ¹J_{CP} = 14 Hz, PCMe$_{min}$), 34.5 (d, ¹J_{CP} = 18 Hz, PCMe$_{maj}$), 34.2 (d, ¹J_{CP} = 21 Hz, PCMe$_{min}$), 31.2 (d, ²J_{CP} = 4 Hz, PC$Me$$_{maj}$), 31.1 (d, ²$J_{CP}$ = 4 Hz, PC$Me$$_{min}$), 30.4 (d, ²$J_{CP}$ = 5 Hz, PC$Me$$_{maj}$), 30.2 (s, NCCH$C$H₂$_{min}$), 30.1 (s, NCCH$C$H₂$_{maj}$), 29.7 (d, ²$J_{CP}$ = 5 Hz, PC$Me$$_{min}$), 25.5 (s, PCCH$C$H₂$_{maj}$), 25.4 (s, PCCH$C$H₂$_{min}$), 21.2 (s, C₆H₂$Me_3$$_{maj}$), 21.1 (s, C₆H₂$Me_3$$_{min}$), 20.8 (s, C₆H₂$Me_3$$_{maj}$), 20.2 (s, C₆H₂$Me_3$$_{min}$), 20.1 (s, C₆H₂$Me_3$$_{min}$), 19.6 (s, C₆H₂$Me_3$$_{maj}$) ppm. ATR-IR (cm⁻¹): 1948 (ν_{CO}), 1879 (ν_{M-H}), 1762 (ν_{M-H}). Anal. Calcd for C₆₁H₇₁AlNOP₃Ru·0.5C₆H₅CH₃ (1101.2): C 70.34, H 6.86, N 1.27; Found C 70.64, H 6.82, N 1.29.

## 2.3. Synthesis of [Ru(IMes)(PPh₃)(CO)H₃{Al(P—N)H}] (4)

A toluene (3 mL) solution of [Ru(IMes)(PPh₃)₂(CO)H₂] (60 mg, 0.061 mmol) and **1** (25 mg, 0.062 mmol) was stirred for 18 h at room temperature in a J. Young's resealable ampoule to afford (by NMR analysis) a mixture of **3** and **4**, and their corresponding diastereomers. The solution was then concentrated by ca. 50% and layered with hexane to give colourless crystals of **4** (31 mg, 45% yield). Redissolution of crystalline material in C₆D₆ for NMR analysis showed that the compound was present as essentially a single diastereomer, given the 4.4:1 ratio of major:minor diastereomers. The NMR data is that for the major diastereomer. ¹H NMR (500 MHz, C₆D₆, 298 K): δ 7.54–6.65 (br, 20H, Ar), 6.43 (s, 1H, Ar), 6.26 (br s, 2H, NCH = CHN), 5.85 (vbr s, 1H, AlH), 3.11 (s, 1H, CN$_{bridge}$H), 2.77 (s, 3H, C₆H₂Me_3), 2.56–2.12 (br, 22H, C₆H₂Me_3 + CP$_{bridge}$H), 1.83–1.64 (m, 2H, CH_2), 1.59 (d, ³J_{HP} = 12.5 Hz, 10H, CMe_3 + CH_2), 1.36 (d, ³J_{HP} = 12.9 Hz, 9H, CMe_3), 1.31–1.27 (m, 5H, C₆H₂Me_3 + CH_2), 1.06 (br d, J = 7.8 Hz, 1H, CH_2), −8.00 (br s, 1H, RuHAl), −10.00 (br d, ²J_{HP} = 65.9 Hz, 1H, RuHAl), −11.26 (br s, 1H, RuHAl) ppm. Selected ¹H NMR (400 MHz, C₆D₅CD₃, 248 K): δ 2.79 (s, 3H, C₆H₂Me_3), 2.50 (s, 3H, C₆H₂Me_3), 2.41 (s, 3H, C₆H₂Me_3), 2.39 (s, 3H, C₆H₂Me_3), 2.38 (s, 3H, C₆H₂Me_3), 2.33 (s, 3H, C₆H₂Me_3), 2.28 (s, 3H, C₆H₂Me_3), 1.42 (s, 3H, C₆H₂Me_3), 1.20 (s, 3H, C₆H₂Me_3) ppm. ³¹P{¹H} NMR (202 MHz, C₆D₅CD₃, 248 K): δ 45.4 (d, J_{PP} = 11 Hz, Ru-PPh₃), −3.1 (br d, J_{PP} = 11 Hz, Al-P) ppm. ¹³C{¹H}NMR (126 MHz, C₆D₆, 298 K): δ 205.5 (d, ²J_{CP} = 11 Hz, Ru-CO), 194.0 (m, Ru-C_{NHC}), 181.0 (d, J_{CP} = 23 Hz, NCCH), 145.4 (d, J_{CP} = 2 Hz, NC_{ipso}Mes), 137.3 (s, C_{quat}Mes), 136.2 (s, C_{quat}Mes), 131.8 (s, C_{quat}Mes), 134.3 (d, J_{CP} = 13 Hz, CH), 134.0 (d, J_{CP} = 13 Hz, CH), 132.6 (s, C_{quat}Mes), 130.8 (s, CH), 129.3 (d, CH), 129.0 (s, CH), 128.8 (s, CH), 128.3 (s, CH), 82.0 (d, ¹J_{CP} = 35 Hz, PCCH), 47.9 (br s, CHCH₂CH), 44.9 (d, J_{CP} = 3 Hz, NCCH), 44.3 (d, J_{CP} = 8 Hz, PCCH), 36.2 (d, ¹J_{CP} = 12 Hz, PCMe), 34.5 (d, ¹J_{CP} = 16 Hz, PCMe), 31.9 (d, ²J_{CP} = 3 Hz, PCMe), 30.5 (d, ²J_{CP} = 5 Hz, PCMe), 30.3 (s, NCCHCH₂), 25.6 (s, PCCHCH₂), 21.3 (s, C₆H₂Me_3), 21.1 (s, C₆H₂Me_3), 20.9 (s, C₆H₂Me_3), 19.2 (s, C₆H₂Me_3) ppm. ATR-IR (cm⁻¹): 1937 (ν_{CO}), 1856 (ν_{M-H}), 1758 (ν_{M-H}). Despite multiple attempts, no satisfactory elemental analysis could be obtained; only values consistent with extensive degradation of the compound were found (e.g. Anal. Calcd for C₆₄H₈₀AlN₃OP₂Ru (1097.3): C 70.05, H 7.35, N 3.83; Found C 47.00, H 3.70, N 1.82).

2.4. Attempted reactions of 1 and other ruthenium hydride precursors

[Ru(PPh₃)(dppp)(CO)H₂] (15 mg, 0.019 mmol) and **1** (7 mg, 0.018 mmol) were combined in C₆D₆ (0.5 mL) in a J. Youngs resealable NMR tube and the sample heated at 60 °C. Monitoring by ¹H and ³¹P{¹H} NMR spectroscopy showed no changes to the spectra over 5 days of heating.

[Ru(PPh₃)₃(CO)HCl] (20 mg, 0.021 mmol) and **1** (9 mg, 0.023
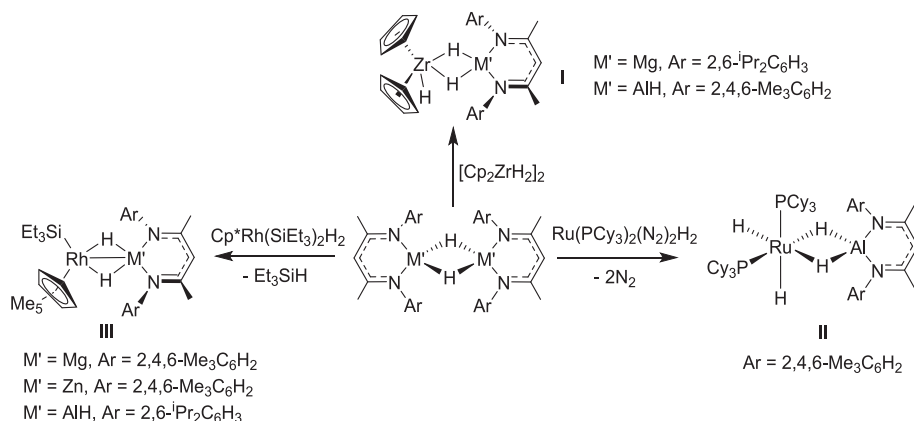
Scheme 1. Recently reported reactions of transition metal hydrides with main group metal hydrides.

mmol) were combined in C_6D_6 (0.5 mL) in a J. Youngs resealable NMR tube, which was shaken at room temperature. ^1H and $^{31}P\{^1H\}$ NMR spectra recorded after 30 min showed conversion to [Ru(PPh$_3$)$_3$(CO)H$_2$]. Addition of a further 0.5 equiv **1** and heating at 60 °C (3 h) led to the appearance of signals for **2**.

[Ru(IMes)(PPh$_3$)$_2$(CO)HCl] (20 mg, 0.020 mmol) and **1** (8 mg, 0.020 mmol) were combined in C_6D_6 (0.5 mL) in a J. Youngs resealable NMR tube. ^1H and $^{31}P\{^1H\}$ NMR spectra recorded after 15 min showed conversion to a mixture of **3** and **4**. Subsequent workup and crystallisation as detailed for **4** above yielded a structure of **4** containing ca. 8% [Ru (IMes)(PPh$_3$)(CO)H$_3$\{Al(P—N)Cl\}].

[Ru(PPh$_3$)$_3$HCl] (20 mg, 0.022 mmol) and **1** (9 mg, 0.023 mmol) were combined in C_6D_6 (0.5 mL) in a J. Youngs resealable NMR tube and shaken for 10 min. Addition of a second equiv **1** consumed some of the residual Ru precursor at the bottom of the NMR tube, but a third equivalent was needed to consume all of it; after a week at room temperature, the solution was homogeneously brown. The solution was reduced to dryness and redissolved in $C_6D_5CD_3$ for analysis by variable temperature ^1H and $^{31}P\{^1H\}$ NMR analysis. Attempts to crystallise one or more of the species present in solution from toluene/hexane, toluene/ pentane, THF/pentane and fluorobenzene/hexane all proved unsuccessful.

2.5. X-ray crystallography

Data for **2**, **4** and **4**/[Ru(IMes)(PPh$_3$)(CO)H$_3$\{Al(P—N)Cl\}] were collected on an Agilent SuperNova instrument and a Cu-Kα source. All experiments were conducted at 150 K, solved using SHELXT [23] and refined using SHELXL [24] via the Olex2 [25] interface. There is one molecule of the bimetallic complex plus a region of solvent in the asymmetric unit of each of the three structures. The solvent was very smeared in all cases and did not lend itself to disorder modelling without excessive paramaterisation. Hence, it was universally addressed *via* the solvent mask algorithm present in Olex2. Disorder modelling has been performed with the inclusion of appropriate distance and ADP restraints throughout.

In **2**, 63:37 disorder was modelled for C47, C48 and C51, as well as for the mesityl moiety containing C52. The hydride ligands were located and refined without restraints. The highest residual electron density peak in this structure is at a chemically insignificant distance from the aluminium centre. This may suggest a small amount of disorder for this metal (trial refinements indicated this would be in the region of 4%). However, this was not ultimately modelled as the data quality for this twinned sample were not sufficient to suggest that any such disorder treatment of Al1 would be credible. Allowance has been made, in the formula as presented, for four molecules of toluene per unit cell. 80:20 disorder was modelled for the norbornene moiety in **4**. The hydride ligands were located and refined without restraints and the formula, herein, accounts for one molecule of hexane per unit cell. As for **4**, the norbornene moiety in **4**/[Ru(IMes)(PPh$_3$)(CO)H$_3$\{Al(P—N)Cl\}] was also treated for disorder – this time in a 70:30 split. The hydride ligands were also located in this structure and refined without restraints. Once again, the formula, allows for the presence of one molecule of hexane per unit cell. There is 8% [Ru(IMes)(PPh$_3$)(CO)H$_3$\{Al(P—N)Cl\}] present in the crystal structure, which was modelled as 92:08 disorder with H4 of the major product.

2.6. Computational methodology

DFT calculations were run with Gaussian 16 (C.01) [26]. The Al, P and Ru centres were described with the Stuttgart RECPs and associated basis sets [27], and the 6-31G** basis sets were used for all other atoms (BS1) [28,29]. A polarisation function was also added to Al ($\zeta_d = 0.190$) and P ($\zeta_d = 0.387$). Initial BP86 [30,31] optimisations were performed using the 'grid = ultrafine' option, with all stationary points being fully characterised via analytical frequency calculations as minima (all positive eigenvalues).

Natural Bonding Orbital (NBO7) [32] analyses were performed on the BP86/BS1-optmised geometries with a larger basis set (BS2) featuring 6–311++G** on all atoms, with the exception of Ru (aug-cc-pVTZ-PP) within Gaussian 16 (C.01) Quantum Theory of Atoms in Molecules (QTAIM) topological analysis of the electron densities of the computed structures were calculated with AIMAll professional (version 19.10.12) [33] using wavefunction files obtained with Gaussian 16 (C.01) at the BP86 level.

3. Results and discussion

3.1. Synthesis and characterisation of [Ru(L)(PPh$_3$)(CO)H$_3$\{Al(P—N) H\}] (**2**: L = PPh$_3$; **4**: L = IMes)

No reaction was observed between the ruthenium dihydride complex [Ru(PPh$_3$)$_3$(CO)H$_2$] and **1** (1 equiv) in benzene solution at room temperature, whereas heating to 60 °C for 18 h led to the complete consumption of the ruthenium precursor and formation of a single product, [Ru(PPh$_3$)$_2$(CO)H$_3$\{Al(P—N)H\}] **2** (Scheme 2).

Following work up, single crystals of **2** were isolated which yielded the X-ray structure shown in Fig. 1, which showed the presence of a Ru···Al core and four surrounding hydride ligands. The reaction is comparable to that which yields **II** (Scheme 1) in that it involves incorporation of **1** into the coordination sphere of [Ru(PPh$_3$)$_2$(CO)H$_2$], formed upon loss of a Ru-bound PPh$_3$ ligand, rather than elimination of H$_2$ [34–38]. The quality of the X-ray data allowed all four hydrides to be located and refined without restraints. For now, we restrict mention to just H4, which is terminally bound Al-hydride (Al1-H4 = 1.641(6) Å). The nature of the three remaining hydrides is considered in light of DFT calculations below.

The ^1H NMR spectrum of a redissolved crystalline sample of **2** showed a broad resonance at δ 5.37 ppm, indicative of the Al-*H* group, in a 1:1:2 ratio with broad signals at lower frequency (a singlet at δ −8.02 ppm and a more complex resonance centred at ca. δ −9.6 ppm) consistent with ruthenium hydrides. Upon ^{31}P-decoupling, the latter resolved into four signals; two broadened triplets at δ −9.51 ppm and δ −9.62 ppm (1:1 ratio), together with two smaller (both with relative integration of 0.6), broad triplets at δ −9.37 ppm and δ −9.68 ppm, which we attribute to the existence of major and minor diastereomers, shown as **2** and **2′** in Scheme 2. As there was very little change in the appearance of the resonances at ca. δ 5.4 ppm and δ −8.0 ppm between the ^1H and $^1H\{^{31}P\}$ NMR spectra, the signals for **2** and **2′** in these cases must be coincident. The $^{31}P\{^1H\}$ NMR spectrum exhibited two broad resonances close to δ 0 ppm, which we assign to the Al-*P* (given the similarity of chemical shifts to **1** (δ 9 ppm)) [17] of the major and minor diastereomers. The Ru-*P* resonances appeared as a series of overlapping
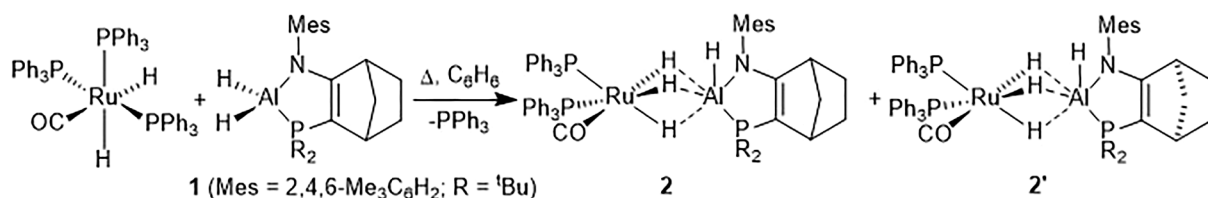
Scheme 2. Synthesis of diastereomers **2** and **2′**.

multiplets at ca. δ 49 ppm; simulation of the spectrum showed the presence of overlapping AB patterns for **2** and **2′**.

In contrast to the elevated temperature required for formation of **2** and **2′**, the *N*-heterocyclic carbene derivative [Ru(IMes)(PPh$_3$)$_2$(CO)H$_2$] (IMes = 1,3-bis-(2,4,6-trimethylphenyl)imidazol-2-ylidene) reacted with **1** at room temperature as evidenced by the ^{31}P{^{1}H} NMR spectrum, which displayed a resonance for free PPh$_3$, as well as four new Ru-PPh$_3$ resonances (δ 52–45 ppm) and four Al-P resonances between δ 5 ppm and δ −3 ppm. The four signals result from the formation of two new products, **3** and **4**, and their accompanying diastereomers **3′** and **4′** (Scheme 3) [39].

Crystallisation yielded colourless crystals of **4** suitable for analysis by X-ray diffraction, as shown in Fig. 2. As with **2**, further consideration of the structure of **4**, [Ru(IMes)(PPh$_3$)(CO)H$_3${Al(P—N)H}], is done in conjunction with computational analysis. NMR spectra arising from redissolved crystalline **4** showed that one diastereomer now dominated (**4**:**4′** = 4.4:1). The ^{1}H NMR spectrum displayed the expected three inequivalent Ru-H signals; broad singlets at δ −8.00 ppm and δ −11.20 ppm, and a broad doublet at δ −10.00 ppm, in a 1:1:1:1 ratio with a very broad Al-H resonance at δ 5.8 ppm. In the ^{31}P{^{1}H} NMR spectrum, the Ru-P and Al-P resonances exhibited a mutual J_{PP} doublet splitting of 11 Hz. There were no significant changes to either the ^{1}H or ^{31}P NMR spectra upon cooling, but warming to above room temperature led to the reappearance of signals from **3**, which suggests that this may be a simple structural isomer of **4**, as shown in Scheme 3. We were unable to confirm this, as all efforts to isolate **3** proved unsuccessful.

3.2. Computational analysis of 2 and 4

Density Functional Theory (DFT) optimised structures of **2** and **4** (BP86/BS1) were subjected to NBO and QTAIM analyses to probe the nature of any interaction between the Ru and Al centres, as well as to better understand the character of the three hydrides H1, H2 and H3 shown in Fig. 3.

A variety of indicators suggested there is very little interaction between the Ru and Al centres in either **2** or **4**. Thus, the frontier molecular orbitals show that the HOMO is concentrated on the Al, P—N ligand and hydride H4, whilst the LUMO was represented by orbitals from the Ru and aryl groups of the PPh$_3$ ligand(s). The computed Ru···Al distances (ca. 2.5 Å; c.f. experimental values of 2.5242(15) Å in **2**, and 2.4806(4) Å in **4**) are on the cusp of the sum of the covalent radii for Ru and Al (2.51 Å [40]; 2.67 Å [41]), but the Wiberg Bond Index (WBI) values of 0.159 (**2**) and 0.166 (**4**) imply an almost negligible covalent interaction between the two centres [42–44]. Analysis of NBO data also confirmed
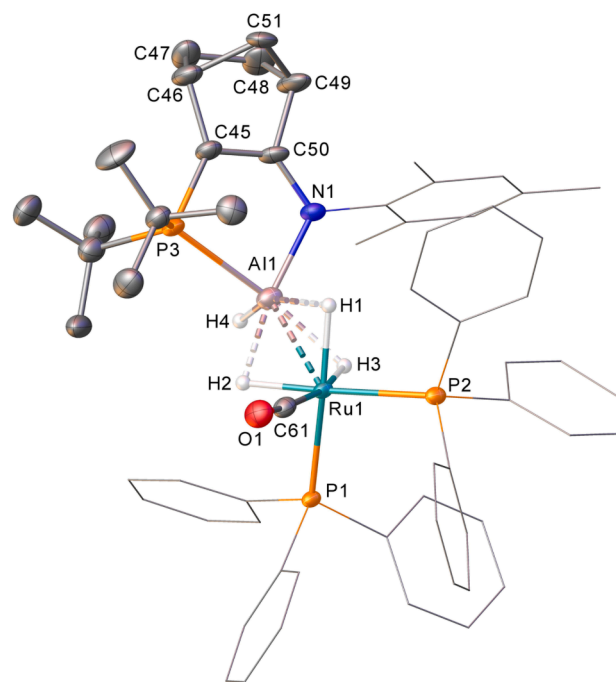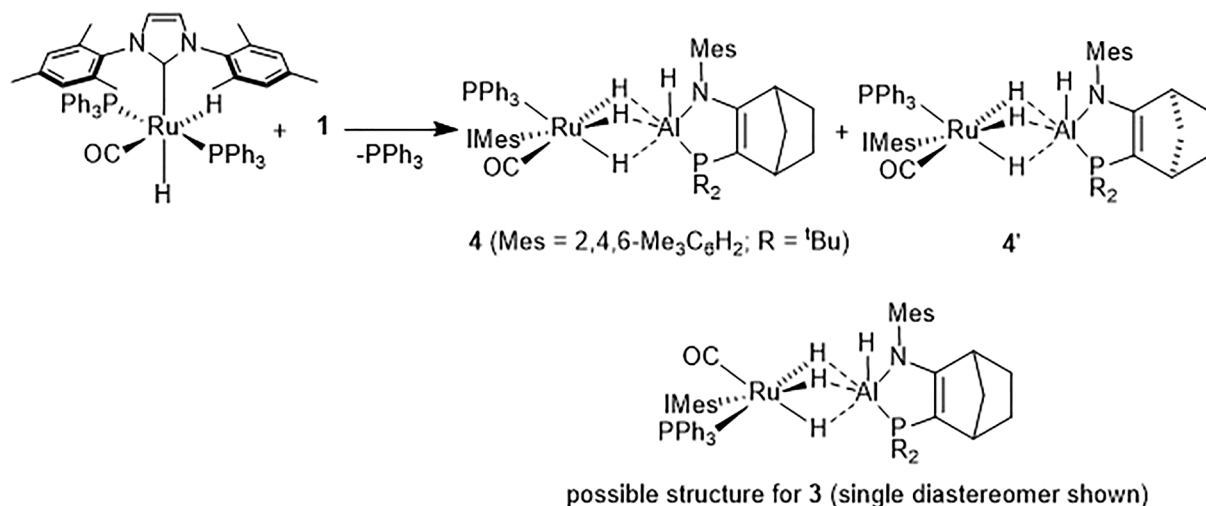

Fig. 1. Molecular structure of **2**. Ellipsoids are represented at 30% probability. Hydrogen atoms, except for the hydrides, have been omitted for clarity. The mesityl group plus the phosphine phenyl rings have been displayed as wireframes and the minor disordered component has been omitted, also for visual ease.

no distinct bonding interactions between Ru and Al. Natural bond charges indicated, unsurprisingly, that the Ru centre was anionic, with q_{Ru} values of −0.88 (**2**) and −0.76 (**4**), whilst the cationic aluminium centre balances this (q_{Al} = +1.07 (**2**) and +1.06 (**4**)) [45]. Although a distinct bond critical point (BCP) was determined by QTAIM calculations along the Ru–Al plane in both **2** (ρ = 0.047) and **4** (ρ = 0.048), the values can be considered as negligible given they are ca. 50% of the size of the BCPs of the Ru-H bonds.

WBI data verified the presence of a single Al-bonded hydride (H4) in **2** and **4**, with negligible H4 interactions to Ru [46]. The three remaining hydrides in both **2** and **4** (NB good agreement was found between experimental and calculated Ru-H···Al distances and angles) show WBI (Ru-H) values in the region of 0.32 to 0.41, compared to the values for WBI(Al-H) which range from 0.23 to 0.30, consistent with their stronger

Scheme 3. Synthesis of diastereomers **4** and **4′**, together with a possible structure for **3**.
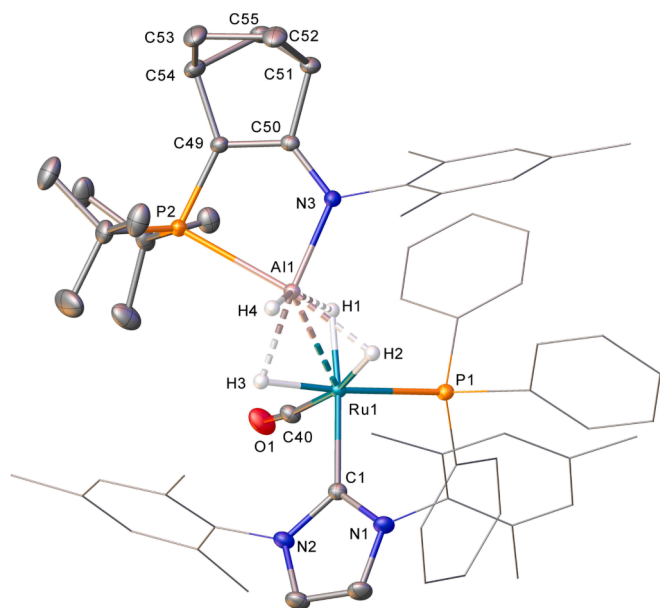
Fig. 2. Molecular structure of **4**. Ellipsoids are represented at 30% probability. Hydrogen atoms, except for the hydrides, have been omitted for clarity. The mesityl groups plus the phosphine phenyl rings have been displayed as wireframes and the minor disordered component has been omitted, also for visual ease.
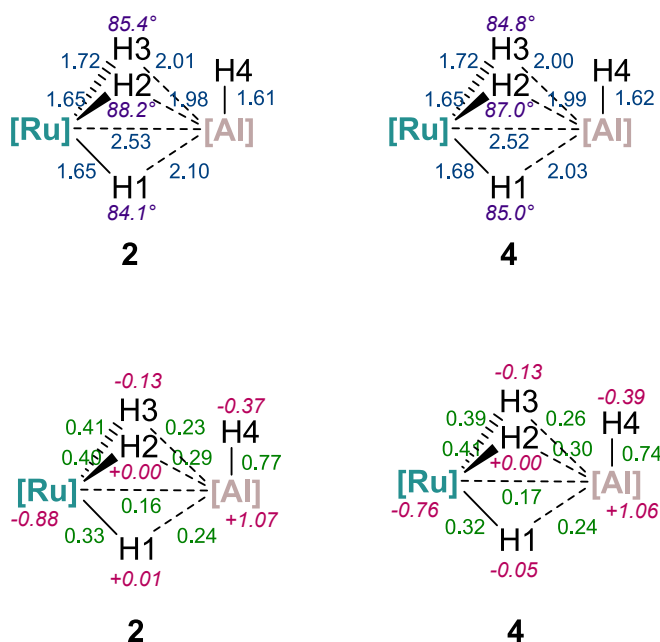

Fig. 3. DFT computed (BP86/BS2//BP86/BS1) parameters of the core Ru, Al and H atoms of complexes **2** and **4** showing (top) bond lengths (Å, dark blue) and angles (°, purple italics) and (bottom) NBO computed charges (pink italics) and Wiberg Bond Indices (green).

association with Ru. Overall, the computational analysis suggests that **2** and **4** are best considered as hydrido ruthenates [Ru(L)(PPh$_3$)(CO)H$_3$]$^-$ [47–49] that interact with a [Al(P—N)H]$^+$ moiety through bridging hydride ligands. Experimental support for this is provided by (i) the observation of J_{PP} coupling between the Ru-*P* and Al-*P* groups in **4**, which clearly establishes connectivity between the two metal centres, (ii) the difference in the NMR data for [Ru(PPh$_3$)$_2$(CO)H$_3$]$^-$ in **2** compared to those reported for the potassium salt [50], that again point

to an active role for [Al(P—N)H]$^+$ and (iii) the solubility of both **2** and **4** in non-polar solvents, such as benzene and toluene [51].

3.3. Reactivity of *1* with other ruthenium hydride precursors

Attempts to extend the reactivity of **1** towards other Ru phosphine hydride precursors yielded mixed results. When [Ru(PPh$_3$)$_3$(CO)H$_2$] was changed to the chelating phosphine derivative [Ru(PPh$_3$)(dppp)(CO)H$_2$] (dppp = 1,3-bis(diphenylphosphino)propane), there was no reaction with **1** even upon heating at 60 °C for 5 days. Thus, it appears that at least two labile PPh$_3$ ligands are required on ruthenium to allow a reaction with **1**. Moreover, it also shows that the desired H$_2$ elimination reaction fails to materialise even when other processes are shut down. Combining **1** and the hydride chloride complex [Ru(PPh$_3$)$_3$(CO)HCl] in a 1:1 molar ratio led to reduction to [Ru(PPh$_3$)$_3$(CO)H$_2$], which then generated **2** upon heating with additional **1**. [Ru(IMes)(PPh$_3$)$_2$(CO)HCl] was also reduced by **1** to [Ru(IMes)(PPh$_3$)$_2$(CO)H$_2$], although the higher reactivity (i.e. lower temperatures) accessed from having an NHC in place of a PPh$_3$ ligand translated into an immediate onwards reaction to form a mixture of **3** and **4**, as well as trace amounts of the chlorido derivative, [Ru(IMes)(PPh$_3$)(CO)H$_3${Al(P—N)Cl}], which was identified as a minor component in an X-ray structure of **4** produced starting from [Ru(IMes)(PPh$_3$)$_2$(CO)HCl].

Addition of up to 3 equiv of **1** to the coordinatively unsaturated hydride precursor [Ru(PPh$_3$)$_3$HCl] yielded multiple broad signals in both the ^{31}P{^{1}H} and low frequency region of the ^{1}H NMR spectra. By analogy to **2** and **4**, these findings suggest that [Ru-H⋯AlH] products form, although we were unable to isolate any crystalline material that allowed unequivocal characterisation.

4. Conclusions

Efforts to prepare heterobimetallic complexes with direct Ru-Al bonds through the combination of [Ru(L)(PPh$_3$)$_2$(CO)H$_2$] (L = PPh$_3$, NHC) precursors with the amidophosphine stabilised aluminium dihydride **1**, and subsequent H$_2$ elimination, yield instead products in which all four hydride ligands are retained and which, on the basis of experimental and computational studies, are best formulated as ruthenates [Ru(L)(PPh$_3$)(CO)H$_3$]$^-$ hydride bridged to [Al(P—N)H]$^+$. Our findings, which are in line with related studies [10,11], point to difficulties in employing H$_2$ loss, as opposed to hydrocarbon elimination, as a way to access TM-MGM heterobimetallic complexes.

CRediT authorship contribution statement

Anne-Frédérique M. Pécharman: Investigation. **Rosalyn L. Falconer:** Investigation. **Esme Owen:** Investigation. **Michael J. Cowley:** Conceptualization. **John P. Lowe:** Investigation. **Claire L. McMullin:** Investigation. **Mary F. Mahon:** Investigation. **Michael K. Whittlesey:** Conceptualization, Writing – review & editing.

Declaration of Competing Interest

The authors declare that they have no known competing financial interests or personal relationships that could have appeared to influence the work reported in this paper.

Data availability

Data will be made available on request.

Acknowledgements

Appendix A. Supplementary data

Supplementary data to this article can be found online at https://doi.org/10.1016/j.poly.2023.116531.

References

[1] F.N. Tebbe, Lewis acidic metal alkyl-transition metal complex interactions. 1. Niobium and tantalum hydrides, J. Am. Chem. Soc. 95 (1973) 5412–5414.

[2] J.N.St. Denis, W. Butler, M. D. Glick, J. P. Oliver, Studies on main group metal-transition metal bonded compounds. II. The crystal and molecular structure of π-$C_5H_5(CO)_3WGa(CH_3)_2$ and evidence for mixed organozinc and organogallium transition metal derivatives, J. Organomet. Chem. 129 (1) (1977) 1–16.

[3] M.D. Fryzuk, D.H. McConville, S.J. Rettig, Fragmentation-recombination reactions of electron-rich binuclear hydride $[P^iPr_2PCH_2CH_2CH_2P^iPr_2)Rh]_2(\mu$-$H)_2$ with dibenzylzinc. X-ray structure of $[P^iPr_2PCH_2CH_2CH_2P^iPr_2)Rh]_2(\mu$-$H)_2(\mu$-$ZnCH_2Ph)_2$, Organometallics 9 (1990) 1359–1360.

[4] R.A. Fischer, D. Weiß, M. Winter, I. Müller, H.D. Kaesz, N. Fröhlich, G. Frenking, The reaction of the group-13 alkyls ER_3 (E = Al, Ga, In; R = CH_2^tBu, CH_2SiMe_3) with the platinum complex $[(dcpe)Pt(H)(CH_2^tBu)]$, J. Organomet. Chem. 689 (24) (2004) 4611–4623.

[5] L. Sotorrios, F.M. Miloserdov, A.F. Pecharman, J.P. Lowe, S.A. Macgregor, M. F. Mahon, M.K. Whittlesey, Zinc-promoted ZnMe/ZnPh exchange in eight-coordinate $[Ru(PPh_3)_2(ZnMe)_4H_2]$, Angew. Chem. Int. Edit. 61 (2022) e202117495.

[6] S. Aldridge, A.J. Downs, Hydrides of the main-group metals: New variations on an old theme, Chem. Rev. 101 (2001) 3305–3365.

[7] M.M.D. Roy, A.A. Omaña, A.S.S. Wilson, M.S. Hill, S. Aldridge, E. Rivard, Molecular main group metal hydrides, Chem. Rev. 121 (20) (2021) 12784–12965.

[8] O. Ekkert, A.J.P. White, H. Toms, M.R. Crimmin, Addition of aluminium, zinc and magnesium hydrides to rhodium(III), Chem. Sci. 6 (2015) 5617–5622.

[9] M.J. Butler, A.J.P. White, M.R. Crimmin, Isomerization of cyclooctadiene to cyclooctyne in a zinc/zirconium heterobimetallic complex, Angew. Chem. Int. Edit. 55 (24) (2016) 6951–6953.

[10] S. Lau, A.J.P. White, I.J. Casely, M.R. Crimmin, Tunable binding of dinitrogen to a series of heterobimetallic hydride complexes, Organometallics 37 (23) (2018) 4521–4526.

[11] T.N. Hooper, S. Lau, W. Chen, R.K. Brown, M. Garçon, K. Luong, N.S. Barrow, A. S. Tatton, G.A. Sackman, C. Richardson, A.J.P. White, R.I. Cooper, A.J. Edwards, I. J. Casely, M.R. Crimmin, The partial dehydrogenation of aluminium dihydrides, Chem. Sci. 10 (35) (2019) 8083–8093.

[12] G. Alcaraz, U. Helmstedt, E. Clot, L. Vendier, S. Sabo-Etienne, A Terminal Borylene Ruthenium Complex: From B−H Activation to Reversible Hydrogen Release, J. Am. Chem. Soc. 130 (39) (2008) 12878–12879.

[13] For examples of H_2 loss from just MGM-H_2 compounds upon reaction with non-hydride containing TM species, see references 14-16.

[14] J. Turner, J.A.B. Abdalla, J.I. Bates, R. Tirfoin, M.J. Kelly, N. Phillips, S. Aldridge, Formation of sub-valent carenoid ligands by metal-mediated dehydrogentaion chemistry: Coordination and activation of $H_2Ga\{(NDippCMe_2)_2CH\}$, Chem. Sci. 4 (2013) 4245–4250.

[15] J.A.B. Abdalla, I.M. Riddlestone, J. Turner, P.A. Kaufman, R. Tirfoin, N. Phillips, S. Aldridge, Coordination and activation of Al-H and Ga-H bonds, Chem. Eur. J. 20 (52) (2014) 17624–17634.

[16] J.A.B. Abdalla, I.A. Caise, C.P. Sindlinger, R. Tirfoin, A.L. Thompson, A.J. Edwards, S. Aldridge, Structural snapshots of a converted double E-H bond activation at a transition metal centre, Nat. Chem. 9 (2017) 1256–1262.

[17] R.L. Falconer, G.S. Nichol, I.V. Smolyar, S.L. Cockroft, M.J. Cowley, Reversible reductive elimination in aluminium(II) dihydrides, Angew. Chem. Int. Ed. 60 (4) (2021) 2047–2052.

[18] H. Samouei, F.M. Miloserdov, E.C. Escudero-Adán, V.V. Grushin, Solid-state structure and solution reactivity of $[(Ph_3P)_4Ru(H)_2]$ and related Ru(II) complexes used in catalysis: a reinvestigation, Organometallics 33 (24) (2014) 7279–7283.

[19] R.F.R. Jazzar, S.A. Macgregor, M.F. Mahon, S.P. Richards, M.K. Whittlesey, C-C and C-H bond activation reactions in N-heterocyclic carbene complexes of ruthenium, J. Am. Chem. Soc. 124 (18) (2002) 4944–4945.

[20] C.W. Jung, P.E. Garrou, Dehydrogenation of alcohols and hydrogenation of aldehydes using homogeneous ruthenium catalysts, Organometallics 1 (4) (1982) 658–666.

[21] N. Ahmad, J.J. Levison, S.D. Robinson, M.F. Uttley, Carbonylchlorohydridotris (triphenylphosphine)ruthenium(II), Inorg. Synth. 15 (1974) 45–48.

[22] R.A. Schunn, E.R. Wonchoba, G. Wilkinson, Chlorohydridotris (triphenylphosphine)ruthenium(II), Inorg. Synth. 13 (1972) 131–134.

[23] G.M. Sheldrick, SHELXT - Integrated space-group and crystal structure determination, Acta Cryst. A A 71 (2015) 3–8.

[24] G.M. Sheldrick, Crystal structure refinement with SHELXL, Acta Cryst. C C 71 (2015) 3–8.

[25] O.V. Dolomanov, L.J. Bourhis, R.J. Gildea, J.A.K. Howard, H. Puschmann, OLEX2: A complete structure solution, refinement and analysis program, J. Appl. Cryst. 42 (2009) 339–341.

[26] M.J. Frisch, G.W. Trucks, H.B. Schlegel, G.E. Scuseria, M.A. Robb, J.R. Cheeseman, G. Scalmani, V. Barone, G.A. Petersson, H. Nakatsuji, X. Li, M. Caricato, A.V. Marenich, J. Bloino, B.G. Janesko, R. Gomperts, B. Mennucci, H.P. Hratchian, J.V. Ortiz, A.F. Izmaylov, J.L. Sonnenberg, D. Williams-Young, F. Ding, F. Lipparini, F. Egidi, J. Goings, B. Peng, A. Petrone, T. Henderson, D. Ranasinghe, V.G. Zakrzewski, J. Gao, N. Rega, G. Zheng, W. Liang, M. Hada, M. Ehara, K. Toyota, R. Fukuda, J. Hasegawa, M. Ishida, T. Nakajima, Y. Honda, O. Kitao, H. Nakai, T. Vreven, K. Throssell, J.A. Montgomery Jr., J.E. Peralta, F. Ogliaro, M.J. Bearpark, J.J. Heyd, E.N. Brothers, K.N. Kudin, V.N. Staroverov, T.A. Keith, R. Kobayashi, J. Normand, K. Raghavachari, A.P. Rendell, J.C. Burant, S.S. Iyengar, J. Tomasi, M. Cossi, J.M. Millam, M. Klene, C. Adamo, R. Cammi, J.W. Ochterski, R.L. Martin, K. Morokuma, O. Farkas, J.B. Foreman, D.J. Fox, Gaussian 16, Revision C.01, Gaussian, Inc., Wallingford CT, 2016.

[27] D. Andrae, U. Häußermann, M. Dolg, H. Stoll, H. Preuß, Energy-adjusted ab initio pseudopotentials for the second and third row transition elements, Theor. Chim. Acta 77 (1990) 123-141.

[28] P.C. Hariharan, J.A. Pople, The influence of polarization functions on molecular orbital hydrogenation energies, Theor. Chim. Acta 28 (3) (1973) 213–222.

[29] W.J. Hehre, R. Ditchfield, J.A. Pople, Self-consistent molecular orbital methods. XII. Further extensions of Gaussian-type basis sets for use in molecular orbital studies of organic molecules, J. Chem. Phys. 56 (5) (1972) 2257–2261.

[30] A.D. Becke, Density-functional exchange-energy approximation with correct asymptotic behavior, Phys. Rev. A 38 (6) (1988) 3098–3100.

[31] J.P. Perdew, Density-functional approximation for the correlation energy of the inhomogeneous electron gas, Phys. Rev. B 33 (12) (1986) 8822–8824.

[32] E.D. Glendening, J.K. Badenhoop, A.E. Reed, J.E. Carpenter, J.A. Bohmann, C.M. Morales, P. Karafiloglou, C.R. Landis, F. Weinhold, NBO 7.0., Theoretical Chemistry Institute, University of Wisconsin (2018).

[33] T.A. Keith, *AIMAll*, vers. 19.10.12: TK Gristmill Software, Overland Park, KS, USA, 2019.

[34] Heating a benzene solution of **2** under 1 atm C_2H_4 at 80 °C resulted in decomposition rather than dehydrogenation of **2**.

[35] It is also worth noting that we found no evidence for attack of **1** on a Ru-CO ligand. For examples where MGM-H reagents and TM-CO precursors react to yield TM-formyl complexes, see references 36-38.

[36] W. Tam, W.-K. Wong, J.A. Gladysz, Neutral metal formyl complexes: Generation, reactivity, and models for Fischer-Tropsch catalyst intermediates, J. Am. Chem. Soc. 101 (1979) 1589–1591.

[37] J. Powell, M.R. Gregg, P.E. Meindl, Synthesis of group 6 metalla-(aza)-crown ether complexes with potentially anionic amido groups. The influence of Li$^+$, Mg^{2+} and Al^{3+} cations on the susceptibility of the carbonyl ligand to nucleophilic addition of alkyl/aryl carbanions and hydride, Organometallics (8) 1989 2942-2947.

[38] J.M. Parr, A.J.P. White, M.R. Crimmin, Magnesium-stabilised transition metal formyl complexes: structures, bonding, and ethenediolate formation, Chem. Sci. 13 (22) (2022) 6592–6598.

[39] There was no effect on the distribution of products if $[Ru(IMes)(PPh_3)_2(CO)H_2]$ was reacted with 2 equiv **1**.

[40] P. Pyykkö, M. Atsumi, Molecular single-bond covalent radii for elements 1–118, Chem. Eur. J. 15 (1) (2009) 186–197.

[41] B. Cordero, V. Gómez, A.E. Platero-Prats, M. Revés, J. Echeverría, E. Cremades, F. Barragán, S. Alvarez, Covalent radii revisited, Dalton Trans. (21) (2008) 2832.

[42] This is supported by the experimental Ru···Al distances in **2** and **4** lying at the upper end of the range for other Ru-*H*-Al systems reported in the Cambridge Crystallograpic Database. Thus, Ru···Al = 2.443(2) Å in $[Ru(PCy_3)_2(N_2)_2H_3\{Al(nacnac)\}]$ (ref 10) and 2.3037(9) Å in $[Ru(PCy_3)(N_2)_2H_4\{Al(nacnac)\}]$ (ref 11). See also references 43-44.

[43] Ru···Al = 2.263(9) and 2.377(11) Å in $[\{Cp^*Ru(\mu$-$H)H(\mu$-$AlCp^*)\}_2]$. T. Cadenbach, T. Bollermann, C. Gemel, R.A. Fischer, Synthesis and structure of electron rich polyhydride complexes and clusters containing AlCp* and GaCp*, Dalton Trans. (2009) 322-329.

[44] T. Steinke, M. Cokoja, C. Gemel, A. Kempter, A. Krapp, G. Frenking, U. Zenneck, R. A. Fischer, C-H activated isomers of $[M(AlCp^*)_5]$ (M = Fe, Ru), Angew. Chem. Int. Ed. 44 (19) (2005) 2943–2946.

[45] The charge differential is slightly larger for complex **2**, where Δq is 1.95, and is reduced to 1.82 in **4**.

[46] For both **2** and **4**, the Al-H4 bond shows contributions of ~ 30 % from Al (s = 41 %, p = 59 %) and 70 % from the H atom.

[47] M. Plois, W. Hujo, S. Grimme, C. Schwickert, E. Bill, B. deBruin, R. Pöttgen, R. Wolf, Open-shell first-row transition-metal polyhydride complexes based on the *fac*-$[RuH_3(PR_3)_3]^-$ building block, Angew. Chem. Int. Ed. 52 (4) (2013) 1314–1318.

[48] M. Plois, R. Wolf, W. Hujo, S. Grimme, Towards reagents for bimetallic activation reactions: Polyhydride complexes with Ru_2H_3, Ru_2ZnH_6, and $Cu_2Ru_2H_6$ cores, Eur. J. Inorg. Chem. 3039–3048 (2013).

[49] A.S.C. Chan, H.-S. Shieh, New synthesis and molecular structure of potassium trihydridotris(triphenylphosphine)ruthenate, J. Chem. Soc. Chem. Comm. (1985) 1379–1380.

[50] W.A. Fordyce, R. Wilczynski, J. Halpern, Hydrido(phosphine)ruthenate complexes and their role in the catalytic hydrogenation of arenes, J. Organomet Chem. 296 (1-2) (1985) 115–125.

[51] D.G. Gusev, A.J. Lough, R.H. Morris, New polyhydride anions and proton-hydride hydrogen bonding in their ion pairs. X-ray crystal structure determinations of Q

[*mer*-Os(H)$_3$(CO)(P^{i}Pr$_3$)$_2$], Q = [K(18-crown-6)] and Q = [K(1-aza-18-crown-6)], J. Am. Chem. Soc. 120 (50) (1998) 13138–13147.